Synthetic Gauge Fields for Vibrational Excitations of Trapped Ions

Alejandro Bermudez,[1,2] Tobias Schaetz,[3,4] and Diego Porras[2]

[1]*Institut für Theoretische Physik, Albert-Einstein Allee 11, Universität Ulm, 89069 Ulm, Germany*
[2]*Departamento de Física Teórica I, Universidad Complutense, 28040 Madrid, Spain*
[3]*Max-Planck-Institut für Quantenoptik, Hans-Kopfermann-Strasse 1, D-85748 Garching, Germany*
[4]*Albert-Ludwigs-Universität Freiburg, Physikalisches Institut, Hermann-Herder-Straße 3, 79104 Freiburg, Germany*

(Received 9 May 2011; published 3 October 2011)

The vibrations of a collection of ions in a microtrap array can be described in terms of tunneling phonons. We show that the vibrational couplings may be tailored by using a gradient of the trap frequencies together with a periodic driving of the trapping potentials. These ingredients allow us to induce effective gauge fields on the vibrational excitations, such that phonons mimic the behavior of charged particles in a magnetic field. In particular, microtrap arrays are well suited to realize a quantum simulator of the famous Aharonov-Bohm effect and observe the paradigmatic edge states typical from quantum-Hall samples and topological insulators.

DOI: 10.1103/PhysRevLett.107.150501 PACS numbers: 03.67.Ac, 37.10.Ty, 37.10.Vz

Introduction.—The ultimate goal of quantum simulation (QS) is to provide an alternative way of exploring the physics of quantum many-body systems [1]. This challenge requires efficient methods to prepare quantum states, an exquisite control of the interactions, and precise measurement techniques. Quantum-information technologies have an important application in this context, since they provide us with a powerful toolbox for the manipulation of quantum systems. In particular, trapped ions [2] are an interesting candidate, their main advantage being an unrivaled efficiency in preparing and measuring quantum states at the single-particle level. In addition, the strong long-range Coulomb interactions make them suitable for the QS of a variety of collective phenomena, from quantum magnetism [3] to dissipative models [4]. So far there have been experiments with up to 9 ions [5], and a lot of effort is being focused on scaling them up. A promising avenue are the so-called two-dimensional arrays of microtraps (2DAM) [6], which may open new routes towards the many-body regime. Unfortunately, this setup still faces some obstacles, such as the large distances between ions ($d_x \approx 40$ μm) leading to weak spin-spin interactions. In order to realize QS schemes based on vibration-mediated interactions, it is fundamental to overcome these issues. Alternatively, focusing directly on the vibrational modes [7] yields a significant speed-up with respect to decoherence rates. In fact, the transfer of vibrational excitations between two aligned traps was recently observed [8].

In this Letter, we show how to tailor the vibrational couplings in a 2DAM, such that this speed-up is exploited. This opens the possibility of building a QS of lattice bosons under synthetic gauge fields. We note that laser-based methods for neutral atoms might also lead to effective gauge fields [9]. Our proposal, however, relies on the different concept of photon-assisted tunneling [10,11], and requires a gradient of the individual trapping frequencies, together with a periodic driving of the trapping potentials that can be achieved by an optical force. This Letter is structured as follows. (i) We show that the amplitude and phase of the vibrational couplings between ions can be tuned by inducing resonances that correspond to the absorption or emission of photons from a classical driving field (photon-assisted tunneling). (ii) We extend this result to 2D and show how it leads to the implementation of synthetic gauge fields, where phonons move like charged particles in a lattice. (iii) We present an implementation of the required drivings by means of optical forces, such that the optical phase can be interpreted as an effective gauge field. (iv) We propose a proof of principle of our ideas with four ions in a plaquette displaying a discrete version of the celebrated Aharonov-Bohm effect [12]. (v) We suggest to concatenate those plaquettes in ladders, leading to Aharonov-Bohm cages [13] and allowing us to observe the edge states characteristic of quantum-Hall samples and topological insulators [14].

(i) Photon-assisted tunneling.—We introduce our scheme for two ions with mass M and charge e, trapped by independent potentials with frequencies $\omega_{1,2}$ [Figs. 1(a) and 1(b)]. The equilibrium positions, separated by d_x, lie along the x direction, and the axial vibrational modes are periodically driven. The Hamiltonian is $H(\tau) = H_0(\tau) + H_c$, with ($\hbar = 1$),

$$H_0(\tau) = \sum_{j=1,2} \omega_j a_j^\dagger a_j + H_d(\tau),$$
$$H_c = \frac{e^2}{d_x^3}(\delta x_1 - \delta x_2)^2. \quad (1)$$

H_c is the Coulomb coupling to second order in the ion displacements, $\delta x_j = (a_j + a_j^\dagger)/\sqrt{2M\omega_j}$, with $a_j^\dagger(a_j)$ phonon creation (annihilation) operators. The periodic driving is

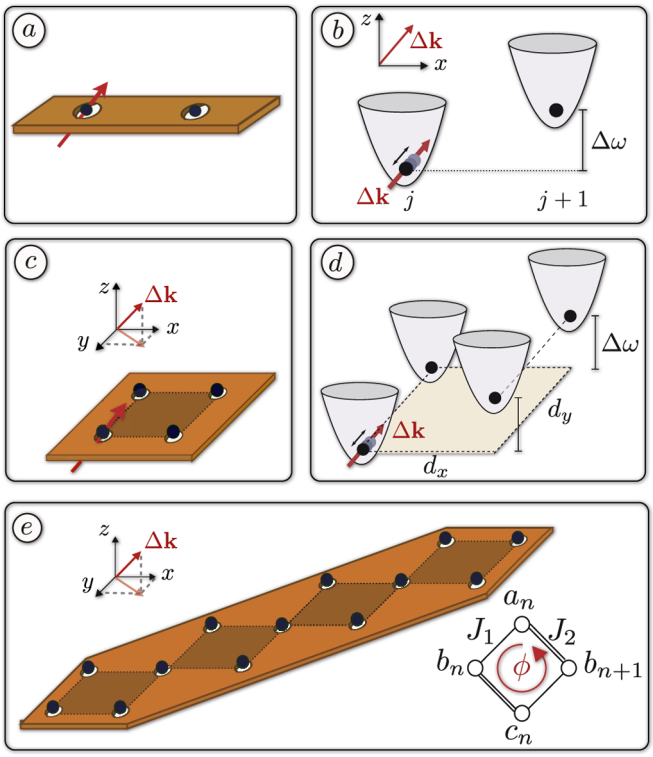

FIG. 1 (color online). Arrangement of ion microtraps: Schematic representation of the microtrap layout for (a) two-ion link, (c) four-ion plaquette, (e) many-ion rhombic ladder [the relevant parameters of the effective Hamiltonian (13) are also shown]. Requirements for the photon-assisted tunneling of phonons: (b) The frequencies of two adjacent traps ω_1, ω_2 are shifted by $\Delta\omega$. By shining a pair of Raman lasers, one assists the phonon transfer. (d) For a plaquette, the gradient is along x and the $\Delta\mathbf{k}$ has a component along the x-y-z axes.

$$H_d(\tau) = \sum_{j=1,2} \eta_d \omega_d \cos(\omega_d \tau + \phi_j) a_j^\dagger a_j, \tag{2}$$

where τ represents the time dependence, ω_d ($\eta_d \omega_d$) is the driving frequency (strength), and ϕ_j a site-dependent phase. We assume that $\omega_1 = \omega$, $\omega_2 = \omega + \Delta\omega$, and $\{\Delta\omega, \eta_d\omega_d\} \ll \omega$; namely, both the frequency difference and driving strength are small perturbations to the trapping frequency. In the absence of driving, the vibrational coupling is

$$H_c = J_c a_2^\dagger a_1 + \text{H.c.}, \tag{3}$$

where $J_c = -\beta\omega$ and $\beta = e^2/M\omega^2 d_x^3$. Equation (3) holds for $|J_c| \ll \omega$, such that the cross terms, $a_1 a_2$, $a_1^\dagger a_2^\dagger$, can be neglected in a rotating-wave approximation (RWA). This condition, which is met for the experiments in [8], allows us to interpret the dynamics as the tunneling of phonons [7].

To understand the effects of driving, we express Eq. (3) in the interaction picture with respect to $H_0(\tau)$, where $a_i(\tau) = a_i e^{-i\omega_i\tau} e^{-i\eta_d \sin(\omega_d\tau+\phi_i)} e^{i\eta_d \sin(\phi_i)}$. After the trivial transformation $a_i e^{i\eta_d \sin(\phi_i)} \to a_i$, one writes $H_c(\tau)$ by replacing the bare Coulomb coupling J_c by a time-dependent dressed coupling

$$J(\tau) = J_c e^{i\Delta\omega\tau} \sum_{s,s'=-\infty}^{\infty} \mathcal{J}_s(\eta_d)\mathcal{J}_{s'}(\eta_d) \times e^{is(\omega_d\tau+\phi_2)} e^{-is'(\omega_d\tau+\phi_1)}, \tag{4}$$

where $\mathcal{J}_s(\eta_d)$ are Bessel functions of the first kind. By choosing the driving frequencies $r\omega_d = \Delta\omega$, with $r = 1, 2, \ldots$, one selects resonant processes that correspond to the absorption or emission of r photons from the classical driving field. If $\Delta\omega \gg J_c$, only the resonant terms must be considered after a RWA, and the effective vibrational coupling can be written as

$$J_{[r]}(\eta_d, \{\phi_n\}) = J_c \mathcal{F}_r(\eta_d, \Delta\phi) e^{-i(r/2)(\phi_1+\phi_2)},$$
$$\mathcal{F}_r(\eta_d, \Delta\phi) = \sum_{s=-\infty}^{\infty} \mathcal{J}_s(\eta_d)\mathcal{J}_{s+r}(\eta_d) e^{i(s+r/2)\Delta\phi}, \tag{5}$$

where $\Delta\phi = \phi_2 - \phi_1$. Since no perturbative assumption is required on the driving strength, the dressed coupling $J_{[r]}$ may be close to the bare one J_c. Figure 2(a) shows a calculation of the dressed coupling under different conditions. By tuning η_d and $\{\phi_j\}$, one controls the amplitude and phase of the tunneling, which may be enhanced or even completely suppressed. We note that the coherent control of tunneling is interesting on its own [10], and can now be investigated with trapped ions.

(ii) Synthetic magnetic fields.—We extend this scheme to different geometries given by the ion equilibrium positions in a 2DAM, separated by d_x, d_y, and labeled by vectors of integers, $\mathbf{i} = (i_x, i_y)$. In the most general situation, trapping frequencies $\omega_{\alpha,\mathbf{i}}$ depend on the site $\mathbf{i}$ and the spatial direction $\alpha = x, y, z$. The trap potentials, together with a driving term, are

$$H_0(\tau) = \sum_{\mathbf{i},\alpha} \omega_{\alpha,\mathbf{i}} a_{\alpha,\mathbf{i}}^\dagger a_{\alpha,\mathbf{i}} + H_d(\tau). \tag{6}$$

The vibrational couplings between ions in the array arise due to the Coulomb interaction

$$V_c = \frac{e^2}{2} \sum_{\mathbf{i}\neq\mathbf{j}} \frac{1}{|\mathbf{r}_\mathbf{i}^0 - \mathbf{r}_\mathbf{j}^0 + \delta\mathbf{r}_\mathbf{i} - \delta\mathbf{r}_\mathbf{j}|}, \tag{7}$$

where $\mathbf{r}_\mathbf{i}^0$ and $(\delta\mathbf{r}_\mathbf{i})_\alpha = (a_{\alpha,\mathbf{i}} + a_{\alpha,\mathbf{i}}^\dagger)/\sqrt{2M\omega_{\alpha,\mathbf{i}}}$ are the equilibrium positions and relative ion displacements. We assume that the vibrational modes in different directions are not coupled and the phonon number is conserved. The validity of this approximation is quantified below. In the harmonic approximation, that is, up to second order in $\delta\mathbf{r}_\mathbf{i}$, we find

$$H_c = \sum_{\mathbf{i}>\mathbf{j},\alpha} J^{\alpha}_{c;\mathbf{i},\mathbf{j}}(a^{\dagger}_{\alpha,\mathbf{i}}a_{\alpha,\mathbf{j}} + a^{\dagger}_{\alpha,\mathbf{j}}a_{\alpha,\mathbf{i}}),$$

$$J^{\alpha}_{c;\mathbf{i},\mathbf{j}} = -\frac{e^2}{2M\sqrt{\omega_{\alpha,\mathbf{i}}\omega_{\alpha,\mathbf{j}}}}\frac{3(\mathbf{r}^0_{\mathbf{i}-\mathbf{j}})_{\alpha}(\mathbf{r}^0_{\mathbf{i}-\mathbf{j}})_{\alpha} - |\mathbf{r}^0_{\mathbf{i}-\mathbf{j}}|^2}{|\mathbf{r}^0_{\mathbf{i}-\mathbf{j}}|^5}, \quad (8)$$

where $\mathbf{r}^0_{\mathbf{i}-\mathbf{j}} = \mathbf{r}^0_{\mathbf{i}} - \mathbf{r}^0_{\mathbf{j}}$. The assumption of independent vibrations in each direction holds for $|\omega_{\alpha,\mathbf{i}} - \omega_{\beta,\mathbf{j}}|_{\alpha\neq\beta} \gg |J^{\alpha}_{c;\mathbf{i},\mathbf{j}}|$, whereas phonon number conservation is valid if $\omega_{\alpha,\mathbf{i}} \gg |J^{\alpha}_{c;\mathbf{i},\mathbf{j}}|$.

In quantum mechanics, charged particles under electromagnetic fields acquire a phase that depends on the field background. To make a QS of this phenomenon, we focus on the ion motion in direction $\bar{\alpha}$ and choose a linear gradient along x, $\omega_{\bar{\alpha},\mathbf{i}} = \omega_{\bar{\alpha}} + \Delta\omega i_x$, together with phases that depend linearly on the position, $\phi_{\mathbf{i}} = \phi_x i_x + \phi_y i_y$. Equation (2) is generalized to $H_d(\tau) = \sum_{\mathbf{i}} \eta_d \omega_d \cos(\omega_d\tau + \phi_{\mathbf{i}})a^{\dagger}_{\bar{\alpha},\mathbf{i}}a_{\bar{\alpha},\mathbf{i}}$. In analogy to the two-ion case, we find that the effective vibrational couplings to leading order in η_d [15] are the following:

$$J^{\bar{\alpha}}_{[r];\mathbf{i},\mathbf{j}} = J^{\bar{\alpha}}_{c;\mathbf{i},\mathbf{j}}\mathcal{F}_r(\eta_d, \Delta\phi_{\mathbf{i},\mathbf{j}})e^{-i(r/2)(\phi_{\mathbf{i}}+\phi_{\mathbf{j}})}\delta_{i_x,j_x+1} + J^{\bar{\alpha}}_{c;\mathbf{i},\mathbf{j}}\delta_{i_x,j_x}, \quad (9)$$

where $\Delta\phi_{\mathbf{i},\mathbf{j}} = \phi_{\mathbf{i}} - \phi_{\mathbf{j}}$, and δ_{i_x,j_x} is the Kronecker delta. The first term describes the photon-assisted tunneling along x, whereas the second one is the bare coupling along y. A crucial result is that the amplitude of tunneling around a plaquette,

$$W^{\bar{\alpha}}_{\circlearrowleft} = J^{\bar{\alpha}}_{[r];\mathbf{i},\mathbf{i}+\hat{\mathbf{y}}}J^{\bar{\alpha}}_{[r];\mathbf{i}+\hat{\mathbf{y}},\mathbf{i}+\hat{\mathbf{x}}+\hat{\mathbf{y}}}J^{\bar{\alpha}}_{[r];\mathbf{i}+\hat{\mathbf{x}}+\hat{\mathbf{y}},\mathbf{i}+\hat{\mathbf{x}}}J^{\bar{\alpha}}_{[r];\mathbf{i}+\hat{\mathbf{x}},\mathbf{i}} = |W^{\bar{\alpha}}_{\circlearrowleft}|e^{i\phi_{\circlearrowleft}},$$

yields an accumulated phase that depends on the laser parameters $\phi_{\circlearrowleft} = -r\phi_y$ and can be recast in terms of the celebrated Aharonov-Bohm phase [12], $\phi_{\circlearrowleft} = e\oint_{\circlearrowleft} d\mathbf{x}\cdot\mathbf{A}$, where $\oint_{\circlearrowleft}$ is the line integral along the plaquette and $\mathbf{A} = r\phi_y y/(ed_x d_y)\hat{\mathbf{x}}$ is a synthetic vector potential. Accordingly, phonons move as charged particles subjected to a magnetic field perpendicular to the microtrap array and yield a bosonic counterpart of the Azbel-Harper-Hofstadter model [16]. We stress that arbitrary fluxes $\phi_{\circlearrowleft} \in [0, 2\pi)$ can be attained, even reaching one flux quantum per unit cell; a regime inaccessible in solid-state materials for realistic magnetic fields. This opens the possibility to observe a dipolar version of the fractal Hofstadter butterfly, among other interesting effects presented in (iv) and (v).

(iii) Realization of the periodic driving.—The simplest setup to realize Eq. (2) would consist of an array of microtraps, where the driving fields are provided by the local control of the electrodes. Since this scheme is yet to be realized and scaled [6,17], we base our alternative approach on state-of-the-art optical forces. We focus on the vibrational modes transverse to the microtrap plane, $\bar{\alpha} = z$, although other schemes along the x-y plane are equally valid [18]. We consider lasers that drive two-photon stimulated Raman transitions between the electronic levels of the ions $|0\rangle_{\mathbf{i}}$, $|1\rangle_{\mathbf{i}}$. The lasers are detuned by ω_L and provide a Raman wave vector $\Delta\mathbf{k}$,

$$H_L = \frac{\Omega_L}{2}\sum_{\mathbf{i}} O_{\mathbf{i}}(e^{i\Delta\mathbf{k}(\mathbf{r}^0_{\mathbf{i}}+\delta\mathbf{r}_{\mathbf{i}})-i\omega_L\tau} + \text{H.c.}), \quad (10)$$

where Ω_L is the Rabi frequency and $O_{\mathbf{i}}$ is an operator acting on the electronic levels. By a proper choice of the laser detunings and polarizations, one may realize $O_{\mathbf{i}} = \mathbf{1}_{\mathbf{i}}$, or other operators like $O_{\mathbf{i}} = \sigma^z_{\mathbf{i}}$ that widen the applicability of our QS (see the section on outlook). The effect of the ion-laser interaction can be understood as a periodic driving of the microtrap frequencies under the assumptions below. We consider a gradient along x, $\omega_{z,\mathbf{i}} = \omega_z + \Delta\omega i_x$, such that the following conditions are fulfilled: $\{\Delta\omega, \omega_L\} \ll \{\omega_{\alpha}, |\omega_{\alpha} - \omega_{\beta}|_{\alpha\neq\beta}\}$. Let us define the Lamb-Dicke parameter along α, $\eta_{\alpha} = |\Delta\mathbf{k}_{\alpha}|/\sqrt{2M\omega_{\alpha}}$. In the limit $\eta_{\alpha} \ll 1$, we perform a Taylor expansion of (10) up to second order in η_{α}, $H_L = H_{L,0} + H_{L,1} + H_{L,2}$. Note that $H_{L,0}$ does not affect the vibrational modes, and $H_{L,1}$ can be neglected if $\Omega_L\eta_{\alpha} \ll \omega_{\alpha}$ in a RWA. This leads to

$$H_{L,2} \approx -\Omega_L\sum_{\alpha,\beta,\mathbf{i}}\eta_{\alpha}\eta_{\beta}O_{\mathbf{i}}\cos(\Delta\mathbf{k}\cdot\mathbf{r}^0_{\mathbf{i}} - \omega_L\tau)a^{\dagger}_{\alpha,\mathbf{i}}a_{\beta,\mathbf{i}}. \quad (11)$$

Finally, by considering $|\omega_{\alpha} - \omega_{\beta}|_{\alpha\neq\beta} \gg \Omega_L\eta^2_{\alpha}$ [18], we neglect the coupling between different directions and get the announced periodic driving presented in Eq. (2) with the following identifications: $\omega_d = \omega_L$, $\eta_d\omega_d = -\Omega_L\eta^2_z$, and $\phi_{\mathbf{i}} = -\Delta\mathbf{k}\cdot\mathbf{r}^0_{\mathbf{i}}$.

Current microtrap design [6,17] is consistent with the above requirements, $\{\omega_{\alpha}, |\omega_{\alpha} - \omega_{\beta}|_{\alpha\neq\beta}\} \gg \{\omega_L, \Delta\omega\} \gg J_{\mathbf{i},\mathbf{j}}$. Typically, $\omega_{\alpha}/2\pi \approx 1$–$10$ MHz, $J/2\pi \approx 5$ kHz. To fit the inequality, we can take $\omega_L/2\pi \approx 50$ kHz. With a typical Lamb-Dicke parameter of $\eta_{\alpha} \approx 0.2$, the condition $\eta_{\alpha}\Omega_L \ll |\omega_{\alpha} - \omega_{\beta}|$ is still fulfilled [18]. In Fig. 2(b), we compare the effective description (5) to the exact optical forces (10) for a two-ion array, with parameters $\Delta\omega = 0.05\omega_z$, $\eta_z = 0.2$, $\Omega_L = 0.75\omega_z$, $\beta = 0.002$, $r = 1$, where the phonon Hilbert space is truncated to $n_{\max} = 4$. We observe an excellent agreement between both descriptions, yielding assisted tunneling for $\Delta\phi \approx \pi$ [10].

(iv) and (v) Aharonov-Bohm physics in lattices.—We apply our ideas to a square lattice and set $r = 1$, $|\Delta\mathbf{k}_x|d_x = 2\pi n_x + \phi_x$, $|\Delta\mathbf{k}_y|d_y = 2\pi n_y + \phi_y$, with $n_x, n_y \in \mathbb{Z}$. The latter are introduced because typical ion distances are larger than optical wavelengths. From Eq. (9), we get the tight-binding model,

$$H_{\text{eff}} = \sum_{\mathbf{i}} J^z_{[1];\mathbf{i},\mathbf{i}+\hat{\mathbf{x}}}a^{\dagger}_{\mathbf{i}}a_{\mathbf{i}+\hat{\mathbf{x}}}e^{-i\phi_{\circlearrowleft}i_y} + \sum_{\mathbf{i},m>0} J^z_{c;\mathbf{i},\mathbf{i}+m\hat{\mathbf{y}}}a^{\dagger}_{\mathbf{i}}a_{\mathbf{i}+m\hat{\mathbf{y}}} + \text{H.c.}, \quad (12)$$

where $\phi_\circlearrowleft = \phi_y$ [19]. Note that photon-assisted tunneling along the diagonals has been neglected, since for $\phi_x = 2\pi - \phi_y$ that tunneling amplitude vanishes $\mathcal{F}(\eta_d, 2\pi) = 0$ [Fig. 2(a)]. Additionally, the remaining diagonal terms, $J^z_{[1];\mathbf{i},\mathbf{i}+\hat{\mathbf{x}}+m\hat{\mathbf{y}}}$, are negligible for $m > 1$ due to the fast dipolar decay.

(iv) Discrete Aharonov-Bohm effect.—The simplest realization of this tight-binding model consists of a single plaquette [Figs. 1(c) and 1(d)]. In Figs. 2(c) and 2(d), we test the validity of the effective dynamics in (12) by comparing with an exact numerical calculation of the complete driven Hamiltonian (10). These results describe a realization of the discrete Aharonov-Bohm effect with minimal required resources. In Fig. 2(d), we observe that an initial excitation can follow two possible paths, either $1 \leftrightarrow 2 \leftrightarrow 3$ or $1 \leftrightarrow 4 \leftrightarrow 3$, enclosing a net flux $\phi_\circlearrowleft = \pi$. The paths interfere destructively and forbid the phonon to tunnel to site 3. Conversely, in Fig. 2(c), phonons tunnel around the plaquette for $\phi_\circlearrowleft = 0$.

(v) Aharonov-Bohm cages and flatband physics.—Let us consider an interesting route beyond the single plaquette, which is the rhombic 3-leg ladder presented in Fig. 1(d). This system is described by the Hamiltonian

$$H = \sum_j J_1(b_j^\dagger a_j + c_j^\dagger b_{j+1}) + J_2(b_j^\dagger c_j + e^{i\phi} a_j^\dagger b_{j+1}) + \text{H.c.}, \tag{13}$$

where we have labeled the boson operators for each leg as a_j, b_j, c_j [Fig. 1(e)]. This Hamiltonian follows directly from Eq. (12), when the plaquettes are arranged along a diagonal, with $J_1 = e^2/(2md_y^3)$, $J_2 = J_1\mathcal{F}_r(\eta_d, \Delta\phi) \times (d_y/d_x)^3$, and $\phi = \phi_y$, $\phi_x = 2\pi - \phi_y$. This model yields two effects. Because of the Aharonov-Bohm interference for $\phi = \pm\pi$, all the modes of the system are localized and one obtains flat vibrational bands [Fig. 2(e)]. In particular, the nonzero energy modes correspond to the so-called Aharonov-Bohm cages, where phonons are not allowed to tunnel two plaquettes apart [13]. Additionally, one finds the so-called edge states, which are midgap modes exponentially localized around the boundaries. By tuning ϕ and J_2/J_1, one can explore a transition between two topologically nonequivalent phases [Fig. 2(f)].

Finally, let us consider the experimental requirements for the implementation of our ideas. The duration of a QS to observe the effects of the synthetic gauge fields is of the order of $1/J_{[r]}$, with $J_{[r]}$ being of the order of the bare

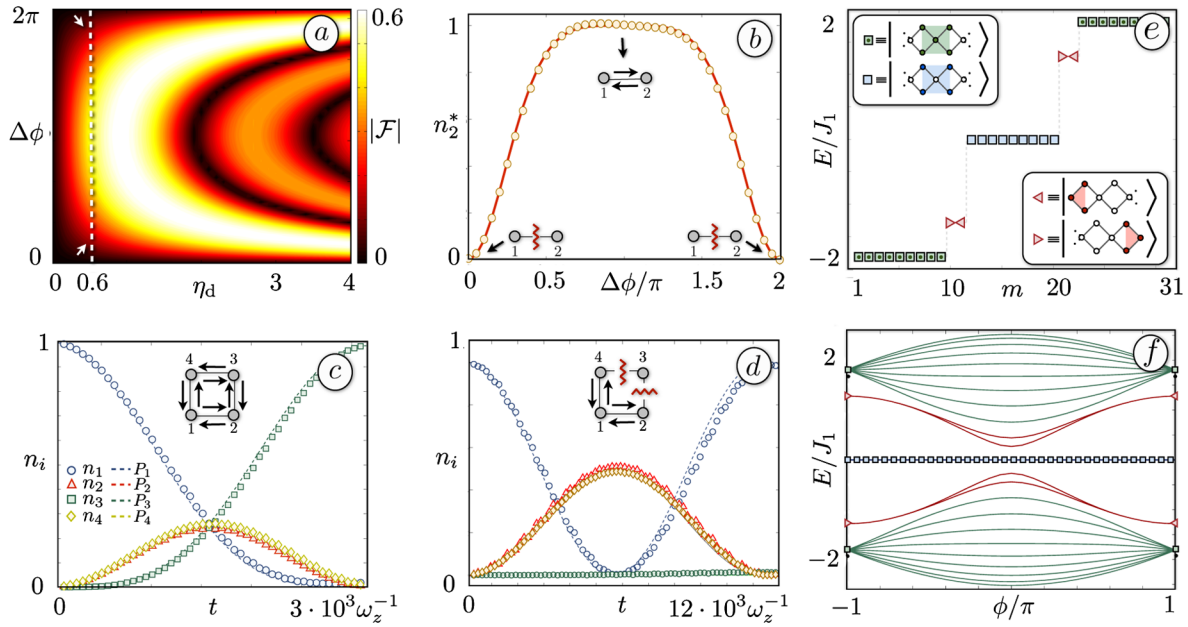

FIG. 2 (color online). Photon-assisted tunneling and Aharonov-Bohm cages. (a) Effective hopping amplitude $|\mathcal{F}_{r=1}|$ as a function of $(\eta_d, \Delta\phi)$. The values of the dashed line at $\eta_d \approx 0.6$ are used in (b). (b) Photon-assisted hopping for a two-ion link of a single vibrational excitation $|\psi_0\rangle = a_1^\dagger|0\rangle$ under the effective description (5) (solid red line) and the complete Hamiltonian (3) with the driving term (10) (yellow dots). We plot the vibrational population n_2^* transferred to site 2 after time $t^* = \pi/|J_{[r]}(0.6, \phi)|$. Maximum phonon transfer occurs at $\Delta\phi = \pi$. (c),(d) Evolution of the phonon excitation in a rectangular plaquette. We plot the phonon populations under approximation (9) $[P_i(t)]$, and under the exact Hamiltonian Eqs. (6)–(8) driven by (10) $[n_i(t)]$. In (c) $\phi_\circlearrowleft = 0$, $\phi_x = \pi$, $\phi_y = 0$, $d_x = d_y|\mathcal{F}_1(\eta_d, \pi)|^{2/3}$, $n_{\max} = 2$, and other parameters same as (b). In (d), $\phi_\circlearrowleft = \pi$, and there is an Aharonov-Bohm destructive interference that inhibits tunneling to site 3. $\phi_x = \pi$, $\phi_y = \pi$, $\Omega_L = 0.25\omega_z$, and other values same as (c). (e) Energy spectrum E for the π-flux regime of Hamiltonian (13) for $N = 31$ microtraps. Flat bands appear at $E \approx \pm 2J_1$ (Aharonov-Bohm cages) (see also the schematic description of the eigenstates), and also at $E = 0$ (which arise solely due to the geometry of the lattice). Also, in the middle of the gaps, single edge states localized to the boundaries of the ladder arise. (f) Energy level spectrum as a function of the effective flux, which displays a gap-vanishing point at $\phi = 0$.

couplings J_c, which are in the range 1–2 kHz [8]. This can be increased to 5 kHz following the trap design [17], and even enhanced by orders of magnitude by further miniaturizing the electrode structure and storing more than one ion per lattice site [8]. The main competing decoherence mechanism is heating of the motional modes [2]. Heating rates as low as 0.07 phonons/ms have been reported in cryogenic traps [8], in principle allowing us to implement our ideas. Even when heating rates are comparable to couplings $J_{[r]}$, they may induce a thermal background over which propagation of vibrational excitations may still be observed [8]. Note that experimental techniques are available for preparation and measurement of phonon states [20]. Also, the vibrational spectrum can be measured without local addressing in the ions' fluorescence sidebands [2].

Conclusions and outlook.—We have presented a proposal to induce synthetic gauge fields for ions in microtrap arrays, which is based on the photon-assisted tunneling of vibrational excitations. By considering trap designs with anharmonicities, effective phonon-phonon interactions can be included [7], which may allow us to study strongly correlated phases. Inducing electronic state-dependent drivings, one gets effective spin-orbit couplings that induce disorder [21]. Also, by adding dissipation, i.e., motional heating, one may study quantum effects in energy transport in the presence of noise [22]. These ingredients make a versatile QS of many-body physics, which would outperform classical computers for ≈ 10 ions and ≈ 4 phonons per ion. That size seems feasible in the near future in view of current experimental progress [6]. Finally, our scheme could be extended to other systems such as photons in arrays of cavities in circuit QED [23].

This work was partially supported by EU STREPs (HIP, PICC), and by QUITEMAD S2009-ESP-1594, FIS2009-10061, CAM-UCM/910758, and RyC Contract No. Y200200074.

[1] R. Feynman, Int. J. Theor. Phys. **21**, 467 (1982).
[2] D. Leibfried *et al.*, Rev. Mod. Phys. **75**, 281 (2003).
[3] D. Porras and J. I. Cirac, Phys. Rev. Lett. **92**, 207901 (2004); A. Friedenauer *et al.*, Nature Phys. **4**, 757 (2008); K. Kim *et al.*, Nature (London) **465**, 590 (2010); E. E. Edwards *et al.*, Phys. Rev. B **82**, 060410 (2010).
[4] J. T. Barreiro *et al.*, Nature (London) **470**, 486 (2011).
[5] R. Islam *et al.*, Nature Commun. **2**, 377 (2011).
[6] T. Schaetz *et al.*, J. Mod. Opt. **54**, 2317 (2007); J. Chiaverini and W. E. Lybarger, Phys. Rev. A **77**, 022324 (2008); J. Labaziewicz *et al.*, Phys. Rev. Lett. **100**, 013001 (2008).
[7] D. Porras and J. I. Cirac, Phys. Rev. Lett. **93**, 263602 (2004).
[8] K. R. Brown *et al.*, Nature (London) **471**, 196 (2011); M. Harlander *et al.*, Nature (London) **471**, 200 (2011).
[9] D. Jaksch *et al.*, New J. Phys. **5**, 56 (2003); see also J. Dalibard *et al.*, arXiv:1008.5378 [Rev. Mod. Phys. (to be published)], and references therein.
[10] M. Grifoni *et al.*, Phys. Rep. **304**, 229 (1998).
[11] A. Eckardt, C. Weiss, and M. Holthaus, Phys. Rev. Lett. **95**, 260404 (2005); C. E. Creffield and T. S. Monteiro, Phys. Rev. Lett. **96**, 210403 (2006); H. Lignier *et al.*, Phys. Rev. Lett. **99**, 220403 (2007); E. Kierig *et al.*, Phys. Rev. Lett. **100**, 190405 (2008).
[12] Y. Aharonov *et al.*, Phys. Rev. **115**, 485 (1959).
[13] J. Vidal, R. Mosseri, and B. Doucot, Phys. Rev. Lett. **81**, 5888 (1998); J. Vidal *et al.*, Phys. Rev. Lett. **85**, 3906 (2000).
[14] M. Z. Hasan *et al.*, Rev. Mod. Phys. **82**, 3045 (2010).
[15] This can be extended straightforwardly to any order of the driving parameter η_d. See A. Bermudez *et al.* (to be published).
[16] M. Ya. Azbel', Zh. Eksp. Teor. Fiz. **46**, 929 (1964) [Sov. Phys. JETP **19**, 634 (1964)].P. G. Harper, Proc. Phys. Soc. London Sect. A **68**, 874 (1955); D. R. Hofstadter, Phys. Rev. B **14**, 2239 (1976).
[17] R. Schmied, J. H. Wesenberg, and D. Leibfried, Phys. Rev. Lett. **102**, 233002 (2009); C. Schneider *et al.*, arXiv:1106.2597.
[18] An effective Raman wave vector along $\hat{z}$ may be obtained without illuminating the trap surface by choosing the trapping axis $\hat{z}$ to be tilted with respect to the surface.
[19] We ignore the x dependence of $\mathbf{A}$ since it may be gauged away by the transformation $a_{\mathbf{i}} \rightarrow a_{\mathbf{i}} e^{-i\chi_{\mathbf{i}}}$, with $\chi_{\mathbf{i}} = \phi_x i_x^2/2$.
[20] D. M. Meekhof *et al.*, Phys. Rev. Lett. **77**, 2346(E) (1996).
[21] A. Bermudez *et al.*, New J. Phys. **12**, 123016 (2010).
[22] M. B. Plenio *et al.*, New J. Phys. **10**, 113019 (2008).
[23] S. Schmidt *et al.*, Phys. Rev. B **82**, 100507(R) (2010).